Chapter 2

Description of the instruments and methods used in study

In the preceding chapter we have already discussed that the high energy radiations like X-ray, gamma rays etc cannot reach the Earth's surface as they get absorbed high up in the atmosphere. So detectors or observatories are needed to place outside the atmosphere in the space to detect these high energy radiations. This is done with the help of sounding rocket, balloon fight and rockets carrying satellites to catch the X-rays coming from different distance sources. The incoming flux of X-ray from the extraterrestrial sources are extremely low, so detector must either have a large photons collecting area so that enough numbers of X-ray photons can be collected for analysis or there must be some kind of X-ray focusing arrangement such that sufficient numbers of X-rays are focused into the detector having reasonable photon collecting area. An astronomical X-ray detectors can have either imaging or non-imaging capabilities. Non-imaging X-ray detectors in principle uses an ionizing capability of X-rays to detect them like in the case of proportional counters, scintillation detector etc and these were used extensively during the early days of X-ray astronomy. However it is not possible to have non-imaging detectors with large collecting area to have timing, spectral and imaging capabilities simultaneously, so in

order to achieve an excellent spectral and imaging capabilities X-ray focusing technique is used. The instruments with imaging capability consist of two parts the telescope to focuses X-rays and the detector. The telescope collects photons from large area and focus these photons on to the detector. However the normal focusing method using mirror or lens will not work for X-ray detection as X-rays can easily penetrate or even ionize the material used in mirror or lens. For this purpose Wolter telescope is used to focus X-rays which is based on the principle of the grazing incidence. The Wolter telescopic arrangement consists of paraboloid mirror followed by hyperboloid mirror. The necessary condition for reflection of X-rays through the telescope is that the angle of incidence of X-ray photons must be of the order of an arc-minutes. This type of telescope is found in the modern day X-ray missions like *CHANDRA, Swift-XRT, NuSTAR* etc. The use of X-ray imaging instruments also help in instantaneous estimations of the background radiations which however, is not possible in a non-imaging detector. Another interesting feature is that it is very helpful in morphological study of the extra-terrestrial X-ray sources.

At about 1000 km above the Earth's surface there exist a region where charged particles are trapped as a result of interaction between charged particle in solar wind and Earth's magnetic field. This region is called *van Allen belt*. Due to this region the X-ray detectors are placed well below the van Allen belt. However due to weakening of magnetic field between South America and South Atlantic region the van Allen belt comes closer to the Earth's surface, less than 500 km from the Earth's surface. This phenomenon is known as *South Atlantic Anomaly* (SAA). So the X-ray detectors onboard satellites must be kept switch off while passing through this region to protect the detectors from being damage.

In this thesis we have used observational data from four space based X-ray observatories namely *RXTE, Swift-XRT, NuSTAR* and *NICER* to study the properties of the neutron star in the X-ray binaries. The brief discussion of the different payloads onboard these observatories are given in the proceeding section.

2.1 Rossi X-ray Timing Explorer *(RXTE)*

The Rossi X-ray Timing Explorer (*RXTE*) is a space borne X-ray observatory named after physicist Bruno Rossi (Fig. 2.1). It was launched on December 30, 1996 which was operational till January 3, 2012. It was designed, built, controlled and managed by NASA Goddard Space Flight Center (GSFC). The mission was able to detect X-rays in 2-250 keV energy range, although its spectral resolution was moderate but it had an excellent time resolution. The two pointed instruments onboard *RXTE* were the Proportional Counter Array (PCA)(Jahoda *et al.*, 1996) and the High Energy X-ray Timing Experiment (HEXTE) (Rothschild *et al.*, 1998), along with these it also consists of a small 1-D coded mask All Sky Monitor (ASM) (Levine *et al.*, 1996).

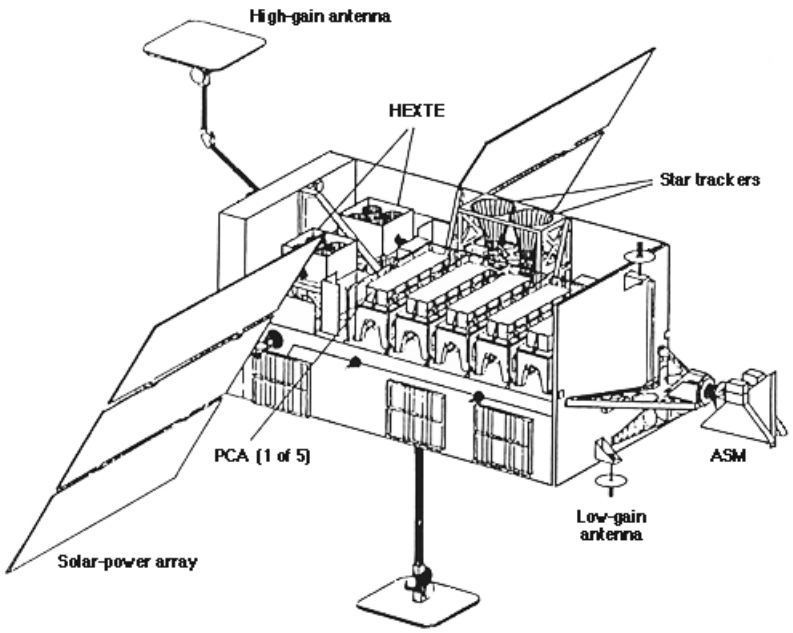

Fig. 2.1 An image of RXTE spacecraft along with different instruments. Image Courtesy: NASA/GSFC

2.1.1 *RXTE*-PCA

The Proportional Counter Array (PCA) was operational in 2-60 keV energy range and it had an energy resolution less than 18% at 6 keV with time resolution about 1 μs. The total collecting area of the PCA was 6500 cm^2. It consist of five identical Proportional Counter Units (PCU). The net geometric collecting area of each PCU was about $\sim$ 1600 cm^2. Each detector consists of two veto layer one at the top and the other at the bottom, there were three more xenon layers each divided into two halfs in between them.

2.1.2 *RXTE*-HEXTE

The High Energy X-ray Timing Experiment (HEXTE) had two clusters (A and B) of detectors, each cluster consist of four NaI(Tl)/CsI(Na)-Phoswich scintillation counters. Each detector was operational in 15-240 keV and had an energy resolution of 15.4% at 60 keV. The net collecting area of HEXTE was about 1600 cm^2.

2.1.3 *RXTE*-ASM

The ASM was used to monitor the sky in 1.5-12 keV energy range. It consists of three Scanning Shadow Camera (SSCs), each of them contains a position-sensitive proportional counter (PSPC). With a total collecting area of 90 cm^2 it was able to scan 80% of the sky in a single revolution. One of the main importance of this instrument was that it was capable of detecting transient X-ray sources in the sky so that the follow-up observation can be carried by the main telescopes of the spacecraft or with other missions.

2.2 Nuclear Spectroscopic Telescope Array *(NuSTAR)*

NuSTAR is the first hard X-ray direct imaging X-ray observatory (Harrison *et al.*, 2013) which was launched successfully on 13 June 2012. It operates in 3-79 keV energy range.

Instead of normal incidence it uses grazing incidence to focus X-rays and this is achieved with the help of two canonical approximation Wolter-I telescopes design optics which focus hard X-rays onto the two solid state detectors placed at the focal plane of the optical device about 10.15 m. away. The two optical devices each contains 133 nested mirror shells, out of these shells the inner 89 shells were coated with depth-graded Pt/C multilayers and the remaining with depth-graded W/Si multilayers and these multilayers reflect efficiently below 79 keV (Pt K-absorption edge). Because of this depth-graded multilayers coating *NuSTAR* it is sensitive to hard X-rays upto 79 keV.

The two telescopes have its own focal plane modulus (FPMA & FPMB) (Fig. 2.2), each focal plane module consists of solid state cadmium zinc telluride (CdZnTe) pixel detector surrounded by a *CsI* anti-coincidence shield. The optical modules are separated from the focal plane modules by a deployable mast. Each detector unit contains four detectors in 2×2 array and each *CdZnTe* detector consists of an array of 32×32, 0.6 mm pixels with each pixel subtending $12.3''$ and thus provides a field of view (FoV) of $12'$ for each focal plane module. The dimension of each *CdZnTe* detector 20mm$\times$20mm with the thickness about 2 mm. The angular resolution (FWHM) of the *NuSTAR* is about $18''$ with energy resolution (FWHM) about 0.4 keV at 10 keV and 0.9 keV at 68 keV. The FoV of the observatory is about $10'$ and $6'$ at 10 and 68 keV respectively. The temporal resolution of the *NuSTAR* is excellent which is about 2 μs. It has a collecting areas 847 cm^2 at 9 keV and 60 cm^2 at 78 keV.

2.3 Swift Observatory (*Swift*)

Swift which is space based laboratory launched on November 20, 2004 is known as Neil Gehrels *Swift* Observatory (Gehrels *et al.*, 2004). It is mostly dedicated to study Gamma Ray Bursts (GRBs). It operates in different wave bands - optical, ultraviolet, X-ray and gamma ray. The study in these different wave bands are done with the help three different

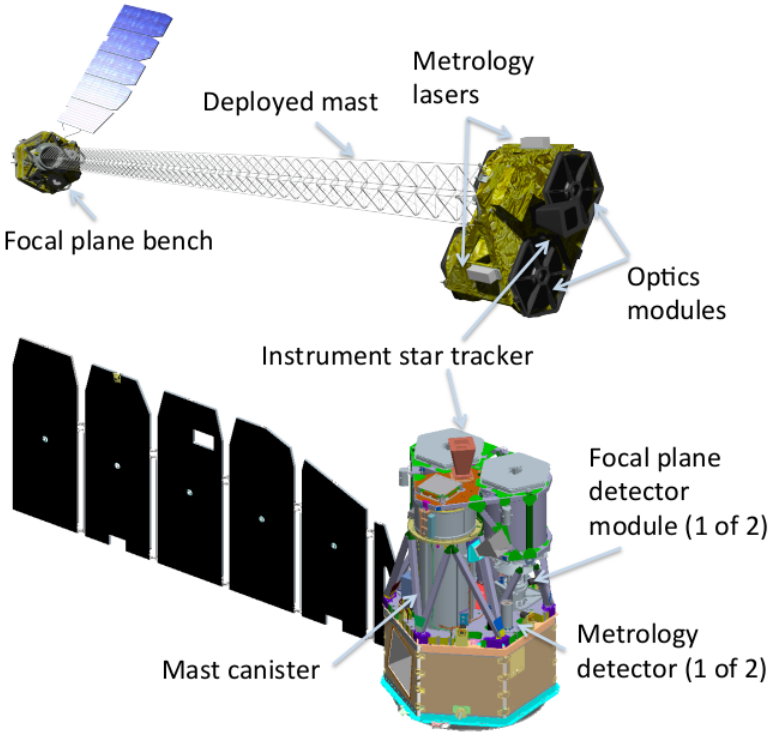

Fig. 2.2 Diagram of the *NuSTAR* observatory. The figures at top and bottom shows the observatory in deployed and stowed configurations respectively. Image courtesy : (Harrison *et al.*, 2013)

instruments - Burst Alert Telescope (BAT), X-ray Telescope (XRT) and Ultraviolet/Optical Telescope (UVOT) (see Fig. 2.3). *Swift*-BAT scans large fraction of sky in search of new GRBs and upon discovery it will trigger the spacecraft to slew automatically to bring burst in the field of views of XRT and UVOT.

2.3.1 *Swift*-BAT

The Burst Alert Telescope (BAT) is one of the three instrument in Swift observatory which consists of a detector plane with coded-aperture mask. The detector plane is made up of 32,768 pieces of CdZnTe hard X-ray detectors each having a dimension of $4\times4\times2$ mm kept 1 m below the coded-aperture mask which is composed of 52,000 pieces of lead each of $5\times5\times1$ mm in size (Barthelmy *et al.*, 2005). It operates in 15-150 keV energy

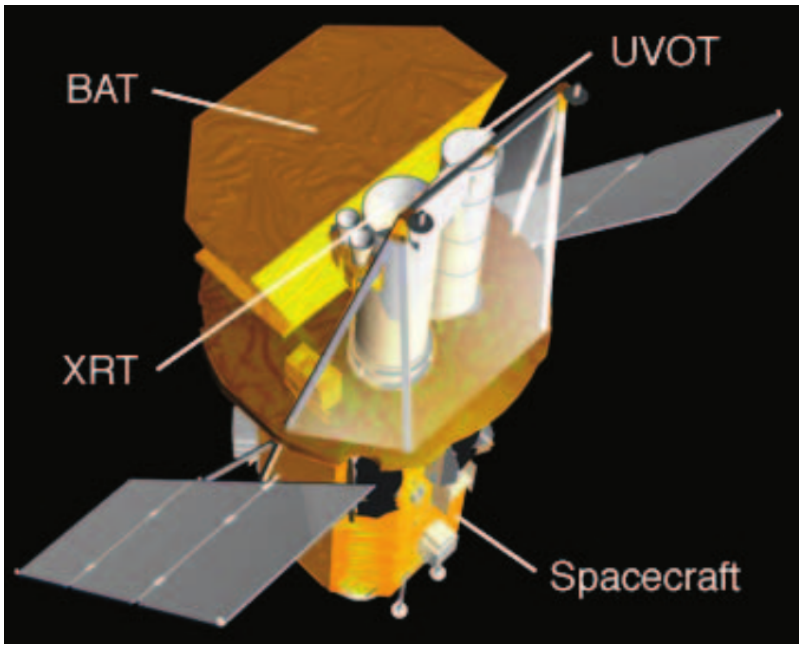

Fig. 2.3 Figure of *Swift* observatory along with different instruments. Image courtesy : (Gehrels *et al.*, 2004)

range having an energy resolution of ∼6 KeV. The FoV of the instrument is about 1.4 sr (half-coded) with a detecting area 5240 cm^2.

2.3.2 *Swift*-XRT

The XRT has two components - mirror module and focal plane camera. Mirror module consists of grazing incidence Wolter I telescope, its focal plane camera consists of a single e2v CCD detector (Burrows *et al.*, 2005). X-rays are focused by the telescope onto the CCD which is thermoelectrically cooled down to - 100^o C. Both the components of the instrument are held in a composite telescopic tube. The XRT can measure the position of the burst with an accuracy of 5 arc-seconds within 100 s of detection of burst by BAT. It operates in 0.2-10 keV energy range and it has an energy resolution of 140 eV at 5.9 keV. The effective area of the instrument is ∼125 cm^2 at 1.5 keV and ∼20 cm^2 at 8.1 keV. Depending on the XRT readout modes the time resolution is between 0.14 ms to 2.5 s.

The FoV of the instrument is about 23.6×23.6 arc-minutes and its detection sensitivity is 2×10^{-14}erg cm^{-2} s^{-1} in 10^4 s.

2.3.3 *Swift*-UVOT

Swift-UVOT uses a modified Ritchey-Chr*e*′tien telescope of 20 cm diameter [1]. The optics and detectors used in it is based on *XMM-Newton*/Optical Monitor (OM). The detectors used in this case are two micro-channel plate intensified CCD (MIC) detectors. These detectors operates in photon counting mode, with its detection capability of very low signal levels which allows UVOT to detect even faint sources over the wavelength 170-650 nm. UVOT has a FoV of 17×17 arcmin having detector element size 2048×2048 pixel.

2.4 Brief review of the sources considered in the study

2.4.1 SMC X-1

SMC X-1 is a 0.71 s X-ray pulsar which is a component of high mass X-ray binary system with a B0 super-giant companion SK 160. The mass of the neutron star companion is about $\sim 17.2M_\odot$ (Reynolds *et al.*, 1993). The detection of the pulsar was first reported by Price *et al.* (1971) when SMC region was examined by rocket flight. It has an orbital period of 3.9 days and is eclipsed for a period ∼0.6 days by its companion (Schreier *et al.*, 1972). The observed luminosity of the source is of the order of 10^{38} erg s^{-1} (Price *et al.*, 1971), near the Eddington limit. The pulsar shows a secular spin-up with a rate of $\sim3.279\times10^{-11}$ Hz s^{-1} (Davison (1977);Wojdowski *et al.* (1998)). The orbital period of the system decayed at a rate of $\sim3.4\times10^{-6}$ yr s^{-1} (Levine *et al.* (1993);Wojdowski *et al.* (1998)). The pulsar also shown a superorbital modulation of about 55-60 days which is thought to be due to the obstruction of X-rays by the precessing accretion disk (Wojdowski

[1] https://swift.gsfc.nasa.gov/about_swift/uvot_desc.html

et al., 1998). From the spin-up rate the predicted magnetic field of the pulsar is $\sim 10^{11}$ G (Li and van den Heuvel, 1997). It undergone a short burst of few tens of seconds which is different from the thermonuclear burst and it may be caused by the viscous instability in the accretion disk. This type of burst is called Type II burst. Angelini *et al.* (1991) were the first to discover this type of burst in SMC X-1. They also observed an aperiodic variability of 0.1 Hz in SMC X-1. The pulsar also shown soft excess which is modelled by a separate blackbody or thermal-bremsstrahlung-type components (Paul *et al.*, 2002). Using *NuSTAR* observations Pike *et al.* (2019) reported the transient pulsation of SMC X-1 and proposed that it is due to partial obscuration of the pulsar by the precessing accretion disk. The source was observed to be varying on the timescales of less than 1 hr (Moon *et al.*, 2003) and its total duration of flares were $\sim$3% of the total observing time. Also these flares are independent of the orbital phases. There are no significant variation in the properties of the pulsars at normal and flare states. Consequently they pointed out that the flare is nothing but simply an extension of the normal state persistent emission with enhanced accretion rates.

2.4.2 Swift J1756.9-2508

Swift J1756.9-2508 was the eighth accreting millisecond X-ray pulsar (AMXP) discovered in 2007 (Krimm *et al.*, 2007a; Markwardt *et al.*, 2007). Accretion millisecond X-ray pulsars are a subclass of low mass X-ray binaries (LMXB) consisting of neutron star having spin period of few milliseconds. The first AMXP SAX J1808.4-3658 was discovered in 1998 using RXTE (Wijnands and van der Klis, 1998). Swift J1756.9-2508 has a spin period of $\sim$5.5 ms and orbital period of 54.7 min. It is a transient in nature and observable during an outburst. The companion of the neutron star is a He-dominated white dwarf having a minimum mass between 0.0067-0.0086$M_\odot$ (Krimm *et al.*, 2007b). After the first outburst in 2007 the second one was observed in 2009 (Patruno *et al.*, 2009b). Patruno

et al. (2010a) observed that the pulse profiles were evolving throughout the outbursts and the pulse fractions of the pulsar are found to increase with the energy even in the hard state. The timing analysis of the 2009 outburst was analyzed by Patruno *et al.* (2010a) and constraint the maximum frequency derivative $\dot{\nu}$ to 3×10^{-13}Hz s^{-1}. Linares *et al.* (2008) reported a strong broad flat topped noise at $\sim$0.1 Hz throughout the 2007 outburst similar to the other AMXPs and LMXBs in the high energy state. The spectrum showed a hard-tail extending upto 100 keV. The 2018 outburst of the source was first detected by *INTEGRAL* (Mereminskiy *et al.*, 2018). Bult *et al.* (2018) studied the long term evolution of orbital period of the AMXP using *RXTE* observations in 2007 and 2009 along with Neutron Star Interior Composition Explorer (NICER) 2018 observations of the outburst and estimated the upper limit of orbital period derivative which is $|P^{\cdot}_{orb}| \leq 7.4\times10^{-13}$s s^{-1}. The estimated magnetic field of the pulsar is of the order of 10^8 G (Patruno *et al.* (2010a);Sanna *et al.* (2018)). During 2018 outburst the source was in hard state with high value of cutoff-energy $\sim$70 keV (Sanna *et al.*, 2018).

2.4.3 4U 1901+03

4U 1901+03 is a $\sim$2.76 s X-ray pulsar which was discovered in 1970-1971 by Uhuru mission but as a X-ray pulsar it was discovered later. After the discovery it was first observed in 2003 during a giant outburst (Galloway *et al.*, 2005). The *RXTE* observations during 2003 outburst revealed that the source is a X-ray pulsar (Galloway *et al.*, 2005). The pulsar is part of a Be X-ray binary (BeXB) system. BeXBs falls under the High Mass X-ray binary (HMXB) system where the companion of the neutron star is a normal Be star (see section 1.3.4). The binary orbital period of the pulsar is about 22.58 days (Galloway *et al.*, 2005). X-ray flares, pulse frequency broadening and quasi-periodic oscillation (QPO) are studied by James *et al.* (2011). QPOs are basically a quasi-periodic signal found in power spectra of the X-ray binaries which is identified by a broad peak

and generally fitted by Lorentzian model. The flares are 100-300s long which are much stronger and more frequent during the peak of an outburst. The QPO was observed around the frequency of $\sim$0.135 Hz having r.m.s. value of 18.5$\pm$3.1 %. It was observed that there were negative residuals near 10 keV in the fitted spectrum observed in the 2003 outburst of the source (Galloway *et al.*, 2005; Reig and Milonaki, 2016), which is known as 10 keV feature. When this feature was fitted with Gaussian absorption model the absorption line was found to show positive correlation with the source luminosity. This feature shows a strong dependence on the pulse phases (Reig and Milonaki, 2016) which points that it can be cyclotron scattering resonance feature (CSRF). The pulse profiles of the pulsar was also varied throughout the outburst (Lei *et al.*, 2009; Reig and Milonaki, 2016) which is due to the change in the beam emission pattern with the luminosity. Lei *et al.* (2009) from the phase-resolved spectroscopy of the pulsar during 2003 outburst found that at the beginning of the outburst the optical depth of the Compton scattering is found maximum near the major peak of the pulse profiles where as during the decay the maximum appears away from the main peak. The outburst of the pulsar was once again detected on February 2019 by MAXI/GSC (Nakajima *et al.*, 2019) and Swift/BAT (Kennea *et al.*, 2019). Ji *et al.* (2020) observed that during the flares it was 1.5 times brighter than the persistent emission. Also the pulse profiles during burst differs from that during normal emission but at the comparable luminosities the pulse profiles have similar shape. In addition to the 10 keV feature an additional 30 keV absorption feature was also observed in the residuals of the source (Coley *et al.*, 2019; Nabizadeh *et al.*, 2020).

2.5 Methods of Data Reduction

The observational data for a given source are obtained from NASA data archive HEASARC. The reduction of these data into useful form were done with the help of the software

HEAsoft[2] which is also provided by HEASARC. Along with the software we also need the updated calibration data base (CALDB) files which are downloaded from the archive. The CALDB files contains the information about the calibration of the high energy astrophysical instruments which is different for different instruments.

We have used 2003 observations of SMC X-1 by *RXTE* in our study. We only consider *RXTE*-PCA data in our study. PCA consist of five unit of PCU, from which we only considered the third unit (PCU2) for analysis. For timing analysis we chose GOODXENON data file, these GOODXENON data are then converted into EVENT data files using the script make_se. These event files are then used to extract light curve of particular binning using the FTOOL seextrct. The FTOOL seextrct is a tool or command which is used to extract light curves and spectra from EVENT mode of *RXTE*-PCA data . For the spectral analysis we used PCA data in STANDARD2 mode which have a binning of 16 s. The data from the top Xe-layer of PCU2 were used to obtain spectra here. The spectra were extracted using saextrct. saextrct is used to create light curves and spectra from *RXTE* SCIENCE ARRAY (SA) data. The background light curves and spectra were obtained using the FTOOL runpcabackest taking the bright source model. The response matrics are to be extracted using pcarsp. The systematic error of 2% was added to all the spectra while fitting them with suitable models. We only consider those data where the elevation of telescope was greater than 10 degree and 30 minutes after the passage from South Atlantic Anamoly (SAA).

For *NuSTAR* observations the standard data screening and filtering will be done using a mission specific FTOOL nupipeline[3]. Through this task we generate cleaned event files from the unfiltered event files. Each Focal plane modules (FPMA & B) has their own event files. A single Level 1 unfiltered event file generates six different Level 2 event files. Out of these six cleaned event files we chose science observing mode (01) event file to extract

[2]https://heasarc.gsfc.nasa.gov/lheasoft

[3]https://heasarc.gsfc.nasa.gov/docs/nustar/analysis/nustar_swguide.pdf

light curves and the corresponding spectra. Using the clean event files we extract source and background region files in XSELECT. The image file extracted in the XSELECT is load in DS9 to see the image. The source region file is chosen to be a circular region around the bright region and another same circular region of same area but far away from the bright region is taken as the background region. After the extraction of the suitable region files the Level3 products *i.e.* light curves and spectra are extracted using nuproducts for each focal plane module. Light curves are background corrected using lcmath and the barycentric correction was done using FTOOL barycorr taking the spacecraft orbit file.

For *Swift/XRT* the reprocessing of unfiltered event file is done with the help of standard task xrtpipeline. The source and background region files are extracted using the same method discussed above. The source and background light curves and spectra are obtained using the respective region files in XSELECT. The ancillary response files (arf) are generated using the tool xrtmkarf, however the response matrics files (rmf) are sourced from the calibration data base files. The background and barycentric corrections are applied using lcmath and BARYCORR respectively.

2.6 Timing and Spectral Analysis

2.6.1 Timing Analysis

Timing analysis of the X-ray pulsars includes study of the light curves, pulse profiles, pulse periods, bursts, quasi-periodic oscillations etc. Thus it provides us with the dynamical properties of the X-ray pulsars. Variation of the pulse periods during the orbital motion of the pulsars due to Doppler effect can be fitted with a suitable model to estimate the orbital parameters. Similarly the study of the pulse profile helps us to figure out the accretion process and accretion geometry. The timing analysis were carried out using timing analysis software XRONOS which comes with HEASoft. In timing analysis we search for the pulse

periods, pulse profile, bursts and energy variation of pulse profiles. Some of the extensively used XORNOS tools are given below,

(i) LCURVE

This XRONOS tool is used to produce light curves, its plots and outputs the results. The light curve shows the variation of the intensity of the pulsar with time. The input file format used is FITS using the BINTABLE extension. At a time up to four simultaneous time series can be input and for more than two input series ratios and sums are calculated. Input data can be rebinned and divided into several intervals and frames. The output plot shows variation of count/s with time and for multiple time series we can also determine colour-colour diagram and hardness ratio.

(ii) POWSPEC

For the crude estimation of the pulse period we perform Fourier transformation of the suitably binned light curve. The frequency corresponding to the pulse period of the pulsar appears as the fundamental peak in the power versus frequency distribution of the Fourier transformation. A XRONOS tool powspec is used for this purpose. This task generates power density spectral (PDS) for one input time series, plots and outputs. The PDS is computed using fast Fourier transformation algorithm or direct slow Fourier algorithm. An input file in FITS format with BINTABLE extension is used. We can rebin the input data and divide it into several intervals and frames. PDS from several intervals can be averaged in a single frame and the results can be rebinned. The output shows the variation of power with frequency. The normalization of the PDS can be changed by changing the value of normalization parameter.

(iii) EFSEARCH

EFSEARCH task is used to search for periodicities in a time series by folding data over a period range and determines the χ^2 of the folded light curve and plots the values of χ^2 with periods. The input file is in FITS format with BINTABLE extension. A guess

value of spin period is required to input in this task, this guess value is estimated using the tool powspec as discussed above. The value of the period where the χ^2 distribution is maximum represents most likely the pulse period of the X-ray pulsar. The error bars of the χ^2 actually the standard deviation of the relevant χ^2 distribution rescale by the χ^2 value for each period divided by N-1, where N is the number of phase bins.

(iv) EFOLD

The efold is a timing tool which creates folded light curves for a given period and the number of phases in the period. The output plot of this folded light curves shows variation of the intensity or count rate with respect to the pulse phase which is known as pulse profiles. It is possible to take upto four input time series simultaneously. The input data can be divided into intervals and frames and folded light curves from different intervals can be averaged in one or more frames. The error bars of the average folded light curves from different intervals are determined using standard deviation of the mean values of each phase bin or propagating the error in each phase. One can set different normalizations for the folded light curve by changing the value of the normalization parameter. For the value of normalization parameter set to 0 we will get folded light curve which are normalised to count/s and if it is set to 1 then the folded light curves are normalised by dividing by the average source intensity in the frame.

2.6.2 Spectral Analysis

Spectral analysis mainly focuses on the study of the continuum shape of the energy spectra of the X-ray pulsars by fitting it with the suitable models. It also includes the study of different emission absorption lines present in the energy spectrum. Spectra are fitted in the X-ray spectral fitting package (XSPEC) (Arnaud, 1996) which is included in HEASoft. Spectra can be fitted also with different models present in the XSPEC. One can create a

simple model using an arithmetic or load local models in it. A detector is used to measure and record the spectrum of a source but its not the actual spectrum whereas its photon count remain within some specific channels. So we need an instrument response file which is proportional to the probability that an incoming photon with some energy E will be detected in channel I, however the instrumental response is continuous which is to be converted into discrete function specific for a given instrument. This is called the detector response matrix. The convolution of the spectrum recorded by the detector with the detector response matrix gives us the energy spectrum of the source. The response matrix is incorporated with the ancillary response file which gives the effective area of the detector. Once we obtain the source and background spectra along with the suitable response files we can fit the background corrected spectrum in XSPEC using the χ^2 method. The test statistic χ^2 is defined as,

$$\chi^2 = \Sigma \frac{(O-M)^2}{\sigma^2}$$

where, O and M are observed and model predicted data photon counts and σ^2 is the variance in the data points. For the goodness of fitting we define reduced χ^2_ν such that,χ^2_ν=χ^2/ν, where ν is the degrees of freedom which is equal to the number of data points minus the number of model parameters. If χ^2_ν=1 then we can say that the model describe the observed spectrum very well. If χ^2_ν>1 then the model is insignificant where as for χ^2_ν<1 the errors is overestimated.

The basic idea behind the spectral analysis is to obtain the value of physical parameter behind the phenomenon which is responsible for the observed spectra. The spectrum of X-ray pulsars are combination of different physical processes which is quite difficult to model the spectra theoretically. As a result the spectra are fitted with empirical model. However the complete model generally is a combination of two or more components of simple or complex mathematical functional form. The general form of the multi-component model

used in fitting spectra is

$$M(E) = Photoelectric\_abs\_model * (cont\_model + emission\_line\_model) * cyc\_line\_model$$

In the next subsection we describe briefly about the models used in the analysis taken up here.

(i) Power law model

The power-law model which is used for absorption is given,

$$M(E) = KE^{-\alpha}$$

where E is the energy, α is photon index and K is model coefficient

(ii) Blackbody model

The blackbody model is given by,

$$M(E) = \frac{K \times 8.0525E^2 dE}{kT^4[exp(E/kT) - 1]}$$

where kT is the temperature in keV and K is the normalization in terms of L_{39}/D_{10}^2, L_{39} is the luminosity in the units of 10^{39} erg/s and D_{10} is the distance to the source in units of 10 kpc.

(iii) Cutoff power law

It is a continuum model consisting power law with high energy exponential roll-off.

$$M(E) = KE^{-\alpha} exp(-E/\beta)$$

where α is the photon index of the power law, β is the e-folding energy of exponential rolloff (in keV) and K is the normalization in photons/keV/cm^2/s at 1 keV.

(iv) High energy cutoff power law

This continuum model consist of power law multiplied by exponential cut-off. One of the form of exponential cutoff model is highecut (White *et al.*, 1983). The high energy cutoff power law model will be used here is given by,

$$M(E) = KE^{-\tau} \times \begin{cases} 1 & E < E_{cut} \\ exp(\frac{E_{cut} - E}{E_{fold}}) & E_{cut} \end{cases}$$

where K and α is the normalization and photon index of the power law model. E_{cut} and E_{fold} are the cutoff energy and e-folding energy in keV of the highecut model.

(v) Gaussian line profile

This model is used to fit the iron line emission in between 6-7 keV energy range. If the width of the model is $\leq$0 then it will be reduced to a delta function. The form of this model is given by,

$$M(E) = K\frac{1}{\sigma\sqrt{2\pi}}exp\left(-\frac{(E-E_l)^2}{2\sigma^2}\right)$$

where E_l is the line energy in keV, σ is the width of the emission line in keV and K is the normalization which represents the total photons/cm^{-2}/s in the line.

(vi) Gaussian absorption line

It is a multiplicative model and widely used to fit the cyclotron absorption line in the spectra of X-ray pulsars. The functional form of the model is given by,

$$M(E) = exp\left(-\frac{\tau}{\sigma\sqrt{2\pi}}exp\left(-\frac{(E-E_a)^2}{2\sigma^2}\right)\right) \tag{2.1}$$

where, E_a is the cyclotron line energy, σ is the line width and τ is the line depth. The optical depth is $\frac{\tau}{\sigma\sqrt{2\pi}}$.

(vii) CompTT

This analytic model describes the Comptonization of soft photons in hot plasma, it is developed by Titarchuk (1994). This model also includes relativistic effects and the approximations fits well for both the optically thick or thin regimes. The model has five parameters - redshift, input soft photon temperature (T_0), plasma temperature (kT), plasma optical depth (τ) and geometry switch. For a disk geometry the geometry switch is ≤ 0 and for spherical one the parameter is >1. The plasma temperature kT and β parameter which does not depends on the geometry completely determines the shape of the Comptonized spectrum. For a given geometry the optical depth is determined by the function β. For the spherical and disc geometry β is not a direct input which is to be frozen. If geometry switch is ≤ 0 then β is obtained from the optical depth using analytical approximation but for geometry switch <0, β is obtained by interpolation from the set of β and τ (Sunyaev and Titarchuk, 1985). The input soft photon spectrum follows Wien law. The plasma temperature lies between 2-250 keV. The model is not valid in the case of simultaneous low temperature and low optical depth or high temperature and high optical depth.

(viii) Photoelectric absorption model

The photoelectric absorption model is described by the function given by,

$$M(E) = exp[-n_H \sigma(E)] \tag{2.2}$$

where $\sigma(E)$ is the photoelectric cross-section which does not include Thomson scattering. In case of phabs photoelectric absorption model the cross-section can be set by using xsect command in XSPEC and the relative abundances are set by the command abund, however

in wabs model uses Wisconsin (Morrison1983) cross-sections along with Anders-Ebihara (Anders and Ebihara, 1982) relative abundance.